Acta Crystallographica Section D
Biological Crystallography
ISSN 0907-4449

Double-stranded helical twisted β-sheet channels in crystals of gramicidin S grown in the presence of trifluoroacetic and hydrochloric acids

Antonio L. Llamas-Saiz,[a]* Gijsbert M. Grotenbreg,[b]‡ Mark Overhand[b] and Mark J. van Raaij[a,c]*

[a]Unidad de Difracción de Rayos X (RIAIDT), Laboratorio Integral de Dinámica y Estructura de Biomoléculas 'José R. Carracido', Edificio CACTUS, Campus Sur, Universidad de Santiago de Compostela, E-15782 Santiago de Compostela, Spain, [b]Leiden Institute of Chemistry, Leiden University, Einsteinweg 55, NL-2333 CC Leiden, The Netherlands, and [c]Departamento de Bioquímica y Biología Molecular, Facultad de Farmacia, Campus Sur, Universidad de Santiago de Compostela, E-15782 Santiago de Compostela, Spain

‡ Current address: Whitehead Institute of Biomedical Research, Cambridge, MA 02142, USA.

Correspondence e-mail: allamas@usc.es, vanraaij@usc.es

Received 18 October 2006
Accepted 28 December 2006

Gramicidin S is a nonribosomally synthesized cyclic decapeptide antibiotic with twofold symmetry (Val-Orn-Leu-D-Phe-Pro)$_2$; a natural source is *Bacillus brevis*. Gramicidin S is active against Gram-positive and some Gram-negative bacteria. However, its haemolytic toxicity in humans limits its use as an antibiotic to certain topical applications. Synthetically obtained gramicidin S was crystallized from a solution containing water, methanol, trifluoroacetic acid and hydrochloric acid. The structure was solved and refined at 0.95 Å resolution. The asymmetric unit contains 1.5 molecules of gramicidin S, two trifluoroacetic acid molecules and ten water molecules located and refined in 14 positions. One gramicidin S molecule has an exact twofold-symmetrical conformation; the other deviates from the molecular twofold symmetry. The cyclic peptide adopts an antiparallel β-sheet secondary structure with two type II′ β-turns. These turns have the residues D-Phe and Pro at positions $i + 1$ and $i + 2$, respectively. In the crystals, the gramicidin S molecules line up into double-stranded helical channels that differ from those observed previously. The implications of the supramolecular structure for several models of gramicidin S conformation and assembly in the membrane are discussed.

1. Introduction

The gramicidins are nonribosomally synthesized peptides that are produced by certain *Bacillus brevis* strains (Dubos, 1939*a*,*b*; Dubos & Cattaneo, 1939). They are antibiotics that act by disrupting biological membranes (Bechinger, 1999; Prenner *et al.*, 1999). Gramicidins A–D are pentadecapeptides which, when crystallized from organic solvents, form double-helical channels with a length that could perceivably cross a biological membrane (reviewed in Burkhart & Duax, 1999). However, NMR and other experiments conducted in lipid environments suggest that the biologically active form is a dimeric single-stranded helical channel (summarized by Anderson *et al.*, 1999; Cross *et al.*, 1999). Crystals grown in the presence of lipids support this notion, although their structure has not been reported (Wallace & Janes, 1991).

Gramicidin Soviet (gramicidin S; Gause & Brazhnikova, 1944) is a cationic cyclic decapeptide antibiotic with twofold symmetry: cyclo-(Val-Orn-Leu-D-Phe-Pro)$_2$ (Schmidt *et al.*, 1957). It has antimicrobial activity against Gram-negative bacteria, Gram-positive bacteria and fungi and also has haemolytic activity against red blood cells (Kondejewski, Farmer, Wishart, Hancock *et al.*, 1996). Its antimicrobial and haemolytic activities are correlated with its ability to destabilize biological membranes, although opinions differ as to whether the two are causally related (Zhang *et al.*, 2001).

Table 1
Crystal data and structure refinement for gramicidin S.

Empirical formula	$3(C_{60}H_{94}N_{12}O_{10})$, $4(C_2F_3O_2H)$, $20(H_2O)$
Formula weight (Da)	4202.51
Temperature (K)	100.0 (1)
Wavelength (Å)	1.5418
Crystal system	Trigonal
Space group	*R*32
Unit-cell parameters (Å, °)	a = 41.4764 (4), b = 41.4764 (4), c = 36.2358 (5), α = 90, β = 90, γ = 120
Volume (Å^3)	53984.7 (10)
Z	9
Density (calculated) (Mg m^{-3})	1.163
Absorption coefficient (mm^{-1})	0.782
Crystal dimensions (mm)	0.75 × 0.08 × 0.05
θ range for data collection (°)	3.47–54.32
Index ranges	$-43 \le h \le 21$, $0 \le k \le 43$, $0 \le l \le 38$
Reflections collected	104642
Independent reflections	7710 (R_{int} = 0.1110)
Completeness to θ = 54.32° (%)	99.7
Absorption correction	Semi-empirical from equivalents
Max. and min. transmission	0.962 and 0.147
Refinement method	Full-matrix least-squares on F^2
Data/restraints/parameters	7710/1575/1273
Goodness-of-fit on F^2	1.864
Final R indices [$I > 2\sigma(I)$]	$R1_{free}$ = 0.1606†, $R1$ = 0.1461, w$R2$ = 0.3849
R indices (all data)	$R1_{free}$ = 0.1682†, $R1$ = 0.1525, w$R2$ = 0.3950
Largest difference peak and hole (e Å^{-3})	0.669 and −0.433

† 5% of the reflections were selected at random for R_{free} calculations.

Various groups are investigating synthetic analogues of gramicidin S, with the ultimate aim of finding an antibiotic that has intact antimicrobial activity but reduced or absent haemolytic properties. Linear analogues of gramicidin S are inactive, while substitution of D-Phe led to reduced activity (Kondejewski, Farmer, Wishart, Hancock *et al.*, 1996). In this work, haemolytic activity was found to closely mirror antimicrobial activity. Changing the ring size has also been tried: cyclic peptides with six or eight amino acids were inactive, whereas 12- or 14-membered rings retained membrane-destabilizing activity. Kondejewski, Farmer, Wishart, Kay *et al.* (1996) reported that 14-residue peptides retain haemolytic but not antimicrobial activity, while 12-residue peptides lost activity against Gram-positive bacteria, retained activity against Gram-negative bacteria and had reduced haemolytic activity. Ando *et al.* (1993, 1995) report somewhat different results for 12- and 14-residue peptides, namely increased antimicrobial activity against Gram-negative bacteria and absence of haemolytic activity. Further studies, reviewed by Lee & Hodges (2003), in which the amphipathicity of gramicidin S analogues was altered, report the generation of cyclic peptides that have high antimicrobial activity and a relatively low haemolytic effect (Jelokhani-Niaraki *et al.*, 2000; McInnes *et al.*, 2000; Prenner *et al.*, 2005) and the development of analogues with a specific activity against certain pathogens (Kondejewski *et al.*, 2002). Recently, Kawai *et al.* (2005) have prepared gramicidin S analogues with extra positively charged substituents on the Pro residues. Activity tests have shown that some of these analogues exhibit reduced haemolysis while maintaining antimicrobial activity. Combined, these works suggest that the antimicrobial and haemolytic activities can be dissociated.

It appears that the presence of cholesterol makes eukaryotic membranes less vulnerable to the action of gramicidin S (Prenner *et al.*, 2001) and thus membrane lipid composition is an important factor in resistance or susceptibility to gramicidin analogues. Studies of membrane interactions of gramicidin S have so far not led to clear conclusions about its mechanism of membrane disruption (reviewed in Prenner *et al.*, 1999). For designing gramicidin S-based antibiotics with the desired properties, a fuller understanding of the mechanism of action of gramicidin S and knowledge of the supramolecular structure that gramicidin S adopts when associated with biological membranes will be valuable.

Here, we report the structure of synthetically obtained native gramicidin S crystallized from a solution containing

Table 2
Selected hydrogen-bond interactions.

Intramolecular interactions are shown in bold. Duplicated values included for comparison purposes are shown in italics. 'Previous structure' refers to that solved by Tishchenko *et al.* (1997).

	Current structure				Previous structure			
Atoms	*D*—H (Å)	H···*A* (Å)	*D*···*A* (Å)	∠(*DHA*) (°)	*D*—H (Å)	H···*A* (Å)	*D*···*A* (Å)	∠(*DHA*) (°)
_A_-Val2 N—H···O _A_-Leu9	**0.88**	**2.11**	**2.939 (9)**	**156.7**	**0.86**	**2.32**	**3.153**	**165.2**
A-Orn3 N—H···O *A*-Pro1[i]	0.88	2.03	2.889 (10)	164.0	No equivalent hydrogen bond			
_A_-Leu4 N—H···O _A_-Val7	**0.88**	**2.06**	**2.912 (13)**	**161.2**	**0.86**	**1.97**	**2.818**	**168.8**
A-Phe5 N—H···O 101 (W)	0.88	2.06	2.94 (2)	177.1	0.86	1.89	2.749	172.4
_A_-Val7 N—H···O _A_-Leu4	**0.88**	**2.19**	**3.045 (14)**	**163.4**	**0.86**	**2.40**	**3.259**	**173.5**
A-Orn8 N—H···O *B*-Orn3	0.88	2.03	2.896 (10)	167.2	No equivalent hydrogen bond			
_A_-Leu9 N—H···O _A_-Val2	**0.88**	**2.01**	**2.872 (9)**	**166.3**	**0.86**	**2.09**	**2.929**	**165.3**
A-Phe10 N—H···O *B*-Pro1	0.88	2.05	2.908 (9)	166.0	No equivalent hydrogen bond			
_B_-Val2 N—H···O _B_-Leu4[ii]	**0.88**	**2.14**	**2.994 (9)**	**164.3**	***0.86***	***2.32***	***3.153***	***165.2***
B-Orn3 N—H···O *A*-Orn8	0.88	2.00	2.868 (9)	167.3	0.86	2.17	3.021	171.1
_B_-Leu4 N—H···O _B_-Val2[ii]	**0.88**	**1.99**	**2.861 (9)**	**168.7**	***0.86***	***1.97***	***2.818***	***168.8***
B-Phe5 N—H···O 102 (W)	0.88	2.18	2.98 (2)	150.3	*0.86*	*1.89*	*2.749*	*172.4*

Current structure		Previous structure	
Atoms	*D*···*A* (Å)	Atoms	*D*···*A* (Å)
A-Orn3 NZ···O *A*-Phe5	2.66 (3)	*A*-Orn3 NZ···O *A*-Phe5	2.77
A-Orn3 NZ···O TFA152[iii]	2.72 (3)		
A-Orn3 NZ···O 105[iii] (W)	3.14 (5)	*A*-Orn3 NZ···O 22 (W)	2.92
A-Orn8 NZ···O *A*-Phe10	2.75 (3)		
A-Orn8 NZ···O 106 (W)	2.89 (5)		
A-Orn8 NZ···O 12 (W)	2.91 (7)		
A-Orn8 NZ···O 111 (W)	2.86 (5)	*A*-Orn8 NZ···O 22 (W)	3.56
A-Orn8 NZ···O 105[iii] (W)	3.08 (5)	*A*-Orn8 NZ···O 23 (W)	3.97
B-Orn3 NZ···O *B*-Phe5	2.66 (2)		
B-Orn3 NZ···O TFA152	2.69 (3)		

Symmetry codes: (i) $x - y, -y, -z$; (ii) $-x + 4/3, -x + y + 2/3, -z + 2/3$; (iii) $y + 2/3, x - 2/3, -z + 1/3$.

water, methanol, trifluoroacetic acid and hydrochloric acid. In the crystals, the gramicidin S molecules line up into double-stranded helical twisted β-sheets. Implications of this supramolecular structure for several models of gramicidin S conformation and assembly in the membrane are discussed.

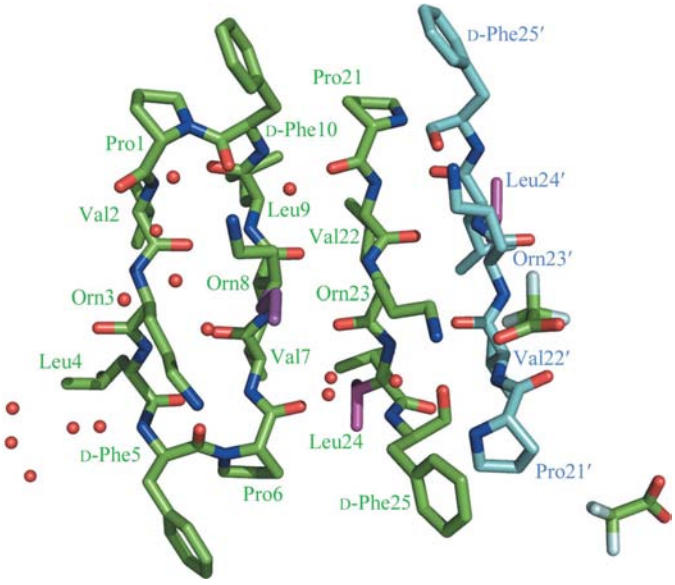

Figure 1
Molecular structure of gramicidin S. The one and a half molecules of gramicidin S present in the asymmetric unit are shown in green; residues are labelled. The twofold symmetry-related half-molecule of gramicidin S is displayed in light blue. The less populated conformations of the disordered side chains of *A*-Orn8 and *B*-Leu4 are displayed in magenta. Water and trifluoroacetic acid molecules are also shown.

2. Materials and methods

2.1. Synthesis, crystallization and data collection of gramicidin S

Gramicidin S was synthesized and purified and its biological activity was assayed as described in Grotenbreg *et al.* (2003). Lyophilized gramicidin S was dissolved to 35 mg ml^{-1} in a 1:1(*v*:*v*) methanol:water mixture, after which 5 µl aliquots of of the solution were pipetted into a 96-well microtitre plate (Terazaki plate) under a layer of *n*-decane. 5 µl of a hydrochloric acid solution was added to the solution (20, 40, 80, 160 or 320 m*M* hydrochloric acid), after which the *n*-decane layer was replaced with mineral oil. The microtitre plate was incubated at 293 K. Crystals of two types developed at all hydrochloric acid concentrations used: prism-shaped crystals belonging to an unidentified primitive monoclinic space group that diffracted to worse than 2 Å resolution and needles belonging to the rhombohedral space group *R*32 that diffracted X-rays to high resolution. A needle-shaped crystal of 0.75 × 0.08 × 0.05 mm was mounted to perform data collection.

2.2. Structure solution and refinement

Intensity data were collected using a Bruker–Nonius FR591 Kappa CCD2000 X-ray diffractometer with Cu $K\alpha$ radiation and multilayer confocal optics by performing eight φ and ω scans (2° oscillations per image) at different κ and 2θ angle settings. The exposure times used were in the range 12–150 s per degree at full-power generator settings (45 kV, 120 mA). Raw images were integrated using *DENZO* (Otwinowski & Minor, 1997) and the resulting intensities were corrected for absorption effects and scaled using *SADABS* (Sheldrick, 2003). Crystal unit-cell parameters were calculated by global refinement using *SCALEPACK* (Otwinowski & Minor, 1997). The structure was solved by direct methods using the program *SnB* v.2.2 (Weeks & Miller, 1999) and refined with no intensity cutoff using the full-matrix least-squares refinement implemented in *SHELXL*97 (Sheldrick, 1998). Throughout the refinement, bond-length, bond-angle and planarity restraints were imposed. All non-H atoms were refined anisotropically with suitable rigid-bond and similarity restraints. H atoms were included as isotropic using a 'riding model' in later stages

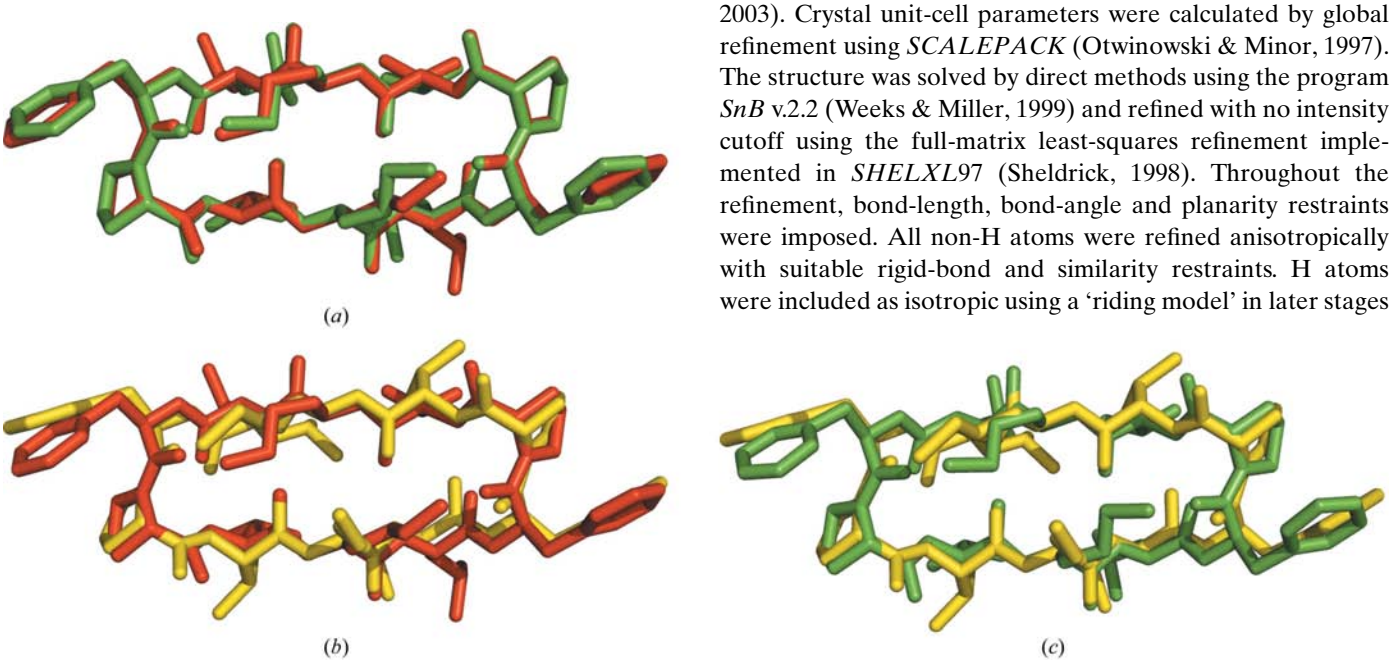

Figure 2
Comparison of the gramicidin S conformations. (*a*) Molecule *A* in red and molecule *B* in green of the current gramicidin S structure. (*b*) Molecule *A* of the current gramicidin S structure (red) and of the previously reported gramicidin S structure (yellow; Tishchenko *et al.*, 1997). (*c*) Molecule *B* of the current gramicidin S structure (green) and the previously reported gramicidin S structure (yellow). Overlays were calculated using the main-chain atoms of the peptides.

of the refinement. A summary of the experimental procedures is gathered in Table 1[1]. Figures were generated using *PyMOL* (DeLano, 2002).

3. Results

The molecular structure of gramicidin S obtained (Fig. 1) is coincident with the Hodgkin–Oughton model proposed almost 50 y ago (Schmidt *et al.*, 1957) and more recently confirmed by Dodson and coworkers (Hull *et al.*, 1978; Tishchenko *et al.*, 1997). The cyclic gramicidin S molecule presents an antiparallel β-sheet secondary structure closed by two type II′ β-turns. This secondary structure is highly stabilized by four strong intramolecular hydrogen bonds involving atoms from the main chain of the Val and Leu residues (Table 2). There are one and a half crystallographically independent peptide molecules, *A* and *B* (Fig. 1). The latter has the molecular C_2 symmetry axis coincident with the crystallographic twofold axis.

The main-chain conformations of the two independent molecules are very similar. The r.m.s. deviation computed for the superposition of the equivalent 40 pairs of main-chain atoms is 0.2 Å (Fig. 2*a*). When all atoms (82) are used to compute the molecular overlay, the r.m.s. difference increases to 1.0 Å (only the most populated side-chain conformations of the disordered residues *A*-Orn8 and *B*-Leu4 were considered). The main differences arise from the side chains of the Leu and Orn residues (Fig. 2*a*). The differences are larger when comparing any of these molecules with the monomer structure previously described by Dodson and coworkers (Tishchenko *et al.*, 1997). The r.m.s. deviations are 0.7 and 0.8 Å for overlays of the main-chain atoms of molecule *A* and *B*, respectively (Figs. 2*b* and 2*c*), and are 1.8 and 1.9 Å when all atoms are included in the same manner as described previously. The principal differences between the main chains of the two gramicidin S structures are in the regions close to the β-turns and lead to stronger intramolecular main-chain hydrogen bonds between the N atoms of the valine residues and the carboxyl O atoms of the leucine residues in the current structure (Table 2). The cause of the differences appears to be the fact that in the current structure the β-sheet formed by the two strands is less twisted. If the twist angle is measured (defined by the relative rotation of lines drawn through the C^{α} atoms of opposing Val and Leu residues in the same molecule), the current structure is shown to have a significantly smaller twist angle than the previously solved structure (18 *versus* 47°). For comparison, the twist angles of the previously reported

Table 3
Geometrical parameters of aromatic π-stacking interactions.

Centroid phenyl ring *A*-Phe5–LSQ plane phenyl ring *A*-Phe10^{i} (Å)	3.3
Centroid phenyl ring *A*-Phe10^{i}–LSQ plane phenyl ring *A*-Phe5 (Å)	3.5
Centroid phenyl ring *A*-Phe5–centroid phenyl ring *A*-Phe10^{i} (Å)	4.067
Slippage (as defined in *PLATON*; Spek, 2003) (Å)	2.055
Shortest intermolecular contact distances (Å)	
A-Phe5 CD2—CE2 *A*-Phe10^{i}	3.355
A-Phe5 CD2—CD2 *A*-Phe10^{i}	3.552
A-Phe5 CG—CG *A*-Phe10^{i}	3.672
A-Phe5 CG—CD2 *A*-Phe10^{i}	3.488
A-Phe5 CD1—CD2 *A*-Phe10^{i}	3.615
A-Phe5 CD1—CG *A*-Phe10^{i}	3.488

Symmetry code: (i) $4/3 - x + y$, $2/3 - x$, $-1/3 + z$.

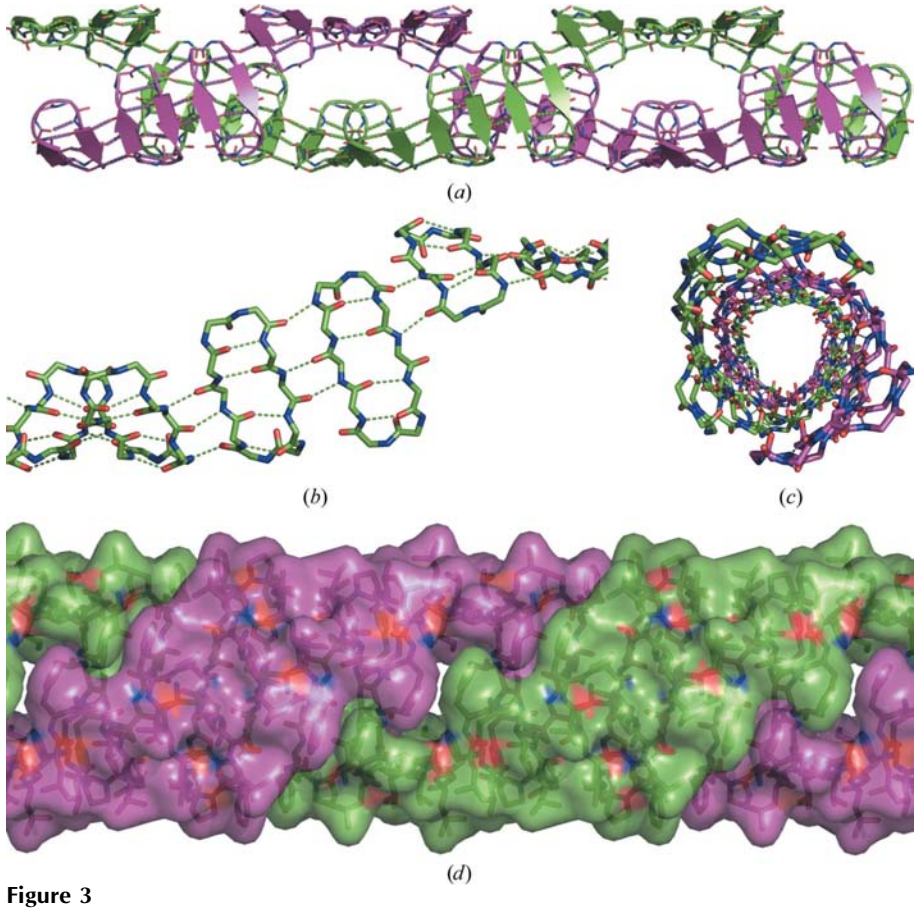

Figure 3
Gramicidin S monomers form double-helical tubes in the crystal with a hydrophobic exterior and hydrophilic interior. (*a*) Schematic diagram of the tube-like organization of the gramicidin S monomer. The two 'ribbons' forming a tube are shown in green and purple, respectively. (*b*) Hydrogen bonds (shown as green broken lines) connect the β-strands along the tube axis. (*c*) Longitudinal view along the channel direction. Both 'ribbons' are shown. (*d*) The ribbons that form the hollow tube are closely packed in the crystal. Stick drawings of gramicidin S monomers surrounded by a transparent envelope representing the molecular surface are shown.

[1] Supplementary data are available from the IUCr electronic archive (Reference: TM5025). Services for accessing these data are described at the back of the journal.

analogues were around 40° (Grotenbreg, Timmer *et al.*, 2004; Grotenbreg *et al.*, 2006).

The monomers give rise to a channel structure formed by two continuous infinite twisted antiparallel β-sheets intertwined in a helical fashion to form a tubular channel (Fig. 3). All the hydrophilic Orn side chains are located in the inner region of the channel, while the Pro, D-Phe, Val and Leu residues form a hydrophobic periphery. Each β-sheet is formed by both crystallographically independent molecules arranged in the series $(ABAABA)_n$. The number of main-chain hydrogen bonds that connect one monomer with the adjacent one is $(3, 3, 2, 3, 3)_n$ (Fig. 3*b* and Table 2). Both β-sheets are packed together through a hydrophobic region comprising all D-Phe side chains (of both molecules *A* and *B*) and the side chain of *A*-Leu4 (Fig. 3*d*). There are also stabilizing π-stacking interactions between the phenyl rings of D-Phe5 and D-Phe10 of molecule *A* (Table 3).

The side chains of *A*-Orn8 and *B*-Leu4 are disordered between two different conformations (Fig. 1). The population ratios refined to 0.70 (2)/0.30 and 0.62 (2)/0.38, respectively. The main conformation of the side chain of *A*-Orn8 is hydrogen bonded to the carbonyl of *A*-D-Phe10, like the other two Orn side chains, residues *A*-Orn3 and *B*-Orn3 (Table 2). No chloride anions have been detected, although hydrochloric acid was included in the crystallization conditions (see §2). It is thus conceivable that the alternative conformation of the Orn side chains, which switch between intramolecular and solvent hydrogen-bond interactions, may be involved in ion conduction inside the channel. The conformational changes modify the inner radius of the channel and the absence of chloride anions in the structure may indicate different protonated states of the ornithine side chains, all of which are properties compatible with passive ion conduction.

Apart from the one and a half gramicidin S molecules found in the asymmetric unit, there are two trifluoroacetic moieties and ten water molecules distributed in 14 locations; 12 are in general positions (six of them with 0.5 occupancies) and the remaining two are in special positions located on crystallographic twofold axes.

4. Discussion

Both in the previously published and in our gramicidin S crystal structures the peptide molecules are arranged following a helical threefold symmetry with additional twofold axes perpendicular to the ternary axis (3_12 symmetry), forming tubular channels (Figs. 3 and 4). However, the overall structures of the three-dimensional channels are very different. In the previous structure, two gramicidin S monomers form twofold-related dimers *via* intermolecular main-chain hydrogen bonds between ornithine residues. Three of these dimers, related by the 3_1 screw axis, give rise to a complete turn of the helical channel. There are no direct hydrogen-bond interactions between the dimers; rather, they are connected by hydrogen bonds through water, methanol and urea molecules and also by regions of hydrophobic interactions (Fig. 4*c*). Therefore, a complete turn of the helical channel comprises six gramicidin S molecules and has a length of 21.5 Å. The channel architecture of the present gramicidin S structure has been described above. In this case, one complete turn of the helical channel contains nine gramicidin S molecules with a length of 36.2 Å, which is potentially sufficient to cross a biological membrane. If the distances from the ornithine CB atoms to the symmetry axis are measured to give an estimation of the inner radii of the channels, the values are 6.2 Å for the previously described structure and 4.7 Å for the present one.

We have previously reported the crystal structures of two furanoid sugar amino-acid analogues of gramicidin S

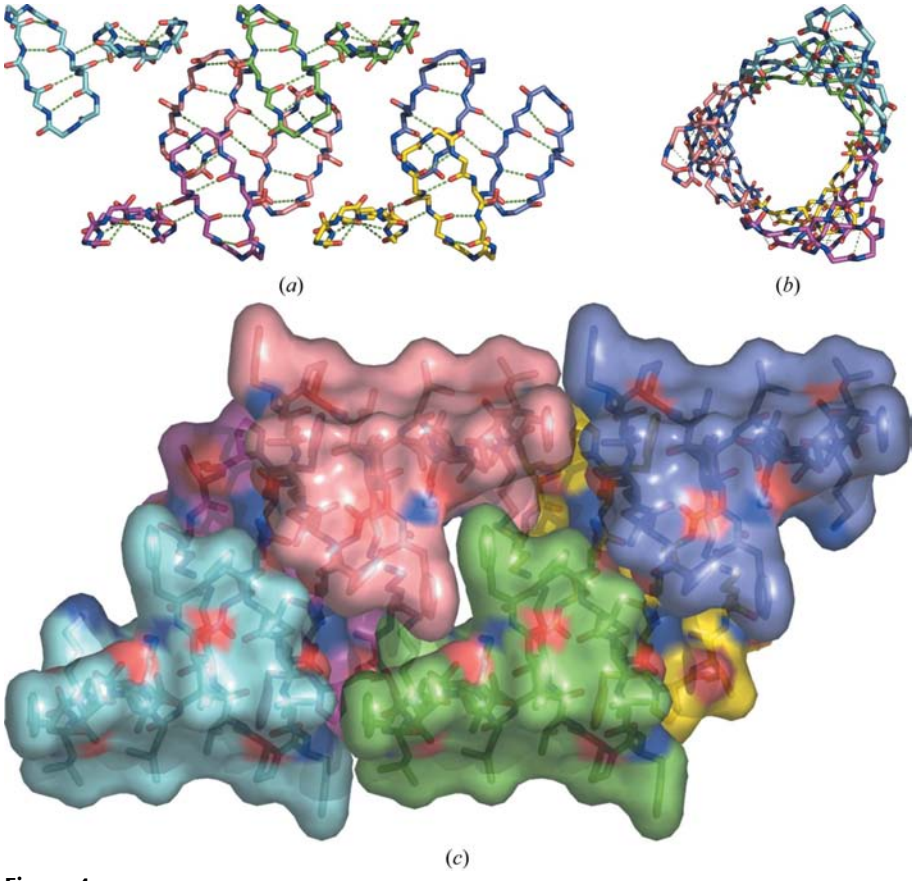

Figure 4
Perpendicular (*a*) and longitudinal (*b*) views of the helical channels in the previously published structure of gramicidin S (Tishchenko *et al.*, 1997). C atoms corresponding to the same hydrogen-bonded dimer are displayed in the same colour. Only main-chain atoms are shown in order to simplify the representation. (*c*) Hydrophobic contacts. All solvent atoms are omitted for the sake of clarity. The colour scheme is the same as in (*a*).

that were synthesized in order to replace one of the native type II′ β-turns by a new reverse turn capable of being the subject of further derivatization. The first, analogue I, contains one sugar amino acid replacing the D-Phe-Pro dipeptide sequence of one of the β-turns; for this analogue, it was found that both the antimicrobial and haemolytic activities were diminished (Grotenbreg, Kronemeijer *et al.*, 2004; Grotenbreg, Timmer *et al.*, 2004). In the second, analogue II, the sugar amino acid was functionalized with an aromatic group, naphthalene, on the C_4-hydroxyl function in order to enhance the mimicry of the analogue towards the original reverse turn of gramicidin S. Antimicrobial and haemolytic activities were completely restored (Grotenbreg *et al.*, 2006). Both gramicidin S analogues form channels in their reported crystal structures, although they are quite different in size and morphology. Analogue I assembles in a hexameric structure corresponding to a 12-stranded β-barrel by two 'sideways' intermolecular hydrogen bonds per monomer. The hexameric units stack on top of each other through one intermolecular hydrogen bond per β-sheet, thus forming channels. Presumably, at least two of these β-barrels (each 13 Å high) stacked on each other would be necessary to cross a lipid bilayer, with one barrel crossing each of the two 15 Å leaflets.

From a previous solid-state nuclear magnetic resonance study in which the leucine residues of gramicidin S were replaced by ^{19}F-phenylglycine, the authors concluded that the cyclic gramicidin S molecule lies flat in the membrane, with the hydrophobic side chains interacting with the lipid tails and the Orn side chains with the phosphate groups (Salgado *et al.*, 2001). These same authors communicated a conference abstract where they observed that during the lipid phase transition, the orientation changes to upright within the lipid bilayer, which is consistent with an oligomeric β-barrel peptide pore in the membrane (Salgado *et al.*, 2000).

Structural studies of the active analogue II revealed that in the crystals 12 gramicidin S molecules form a helical pore with 6_522 symmetry, again with a hydrophilic interior and a hydrophobic exterior (Grotenbreg *et al.*, 2006). Interestingly, all biologically active analogues of gramicidin S and gramicidin S itself, of which two structures have been solved, have helical supramolecular structures.

Regarding the size of the channels, analogue I and analogue II form the channels with the largest pore radii; the estimated values (see above) are 8.3 and 15.0 Å for analogue I and analogue II, respectively. However, for the widest channels formed by analogue II no direct hydrogen bonds between peptide molecules were found. The monomers are joined through a hydrogen-bonded water network and by hydrophobic interactions, mainly among the naphthyl, phenyl and proline rings.

The new channel of gramicidin S described here seems to have the strongest three-dimensional construction along the tube axis, with an average of 2.5 direct hydrogen bonds between the main-chain atoms per monomer. The second strongest could be the stacking of six-membered β-barrels in the gramicidin S derivative analogue I (Grotenbreg, Timmer *et al.*, 2004), with one hydrogen bond per monomer in the direction of the pore. The other two helical channels described for gramicidin S-related compounds, native gramicidin S (Tishchenko *et al.*, 1997) and analogue II (Grotenbreg *et al.*, 2006), do not present any direct hydrogen bonds connecting monomers along the axes of the helical pores. In all four structures there are hydrogen-bonded solvent networks that connect and stabilize the three-dimensional structure.

Our structure and the previously published structure of native gramicidin S both contain double-stranded helical models, comparable to the double-stranded gramicidin A–D structures solved by X-ray crystallography (Fig. 5*a*). However, in the case of gramicidin A–D, studies carried out in lipid environments suggest that two stacked single-helical half-channels constitute the active conformation (Fig. 5*b*). The current model of the interaction of gramicidin S with the membrane is shown schematically in Figs. 5(*c*) and 5(*d*): the hydrophobic side interacts with the lipid chains and the other positively charged side interacts with the phosphates, disturbing the proper alignment of the phospholipids. A model based on the structure of analogue I (Grotenbreg, Timmer *et al.*, 2004) is shown in Fig. 5(*e*). The current Fig. 5(*f*) and the previously solved structures of native gramicidin S suggest a helical pore. As all gramicidin S structures show pores with hydrophilic interiors and hydrophobic exteriors, in principle they are all compatible with a membrane environment. To resolve the question of which structure is biologically relevant, further structural studies in lipid environments should be performed. The elucidation of the supramolecular structure that gramicidin S adopts in different biological membranes

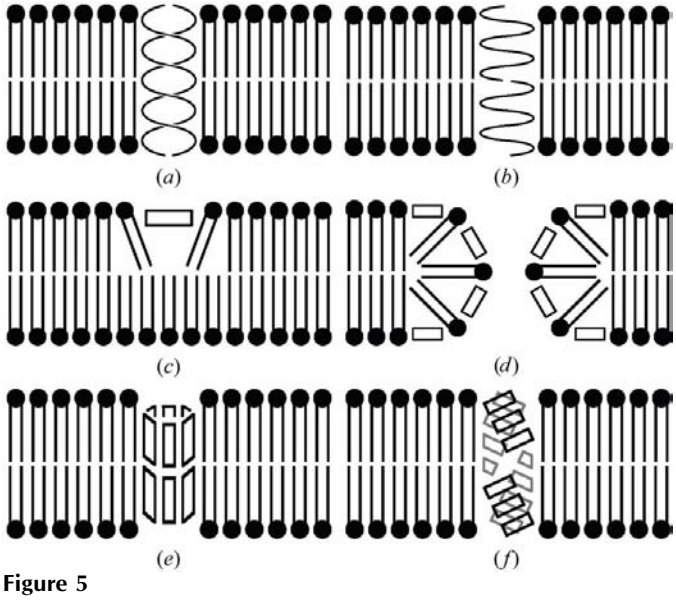

Figure 5
Schematic representations of alternative models of supramolecular gramicidin conformations in a biological membrane. (*a*) Gramicidin A–D intertwined dimers. (*b*) Gramicidin A–D stacked dimer. (*c*) Model of a single amphipathic gramicidin S molecule interacting with the membrane, which could lead to membrane thinning or pore formation [see (*d*) as discussed for other antimicrobial peptides (Huang *et al.*, 2004)]. (*d*) Putative pore formed by multiple gramicidin S molecules interacting with the membrane. (*e*) Two gramicidin S hexamers stacked on top of each other. (*f*) Front view of putative helical gramicidin S pores in the membrane.

should help in the quest for improved gramicidin S-based antibiotics that have antimicrobial properties but lack haemolytic activity.

This research was funded by research grants BMC2002-02436 and BFU2005-02974 from the Spanish Ministry of Education and Science and PGIDIT03PXIC20307PN from the Xunta de Galicia. Further financial support was received from the Council for Chemical Sciences of The Netherlands Organization for Scientific Research (CW-NWO), The Netherlands Technology Foundation (STW) and DSM Research. MJvR is supported by a 'Ramón y Cajal' contract of the Spanish Ministry of Education and Science. The apparatus on which X-ray measurements were performed was co-financed *via* the European Regional Development Fund programme.

References

Anderson, O. S., Apell, H.-J., Bamberg, E., Busath, D. D., Koeppe, R. E. II, Sigworth, F. J., Szabo, G., Urry, D. W. & Woolley, A. (1999). *Nature Struct. Biol.* **6**, 609.

Ando, S., Nishihama, M., Nishikawa, H., Takiguchi, H., Lee, S. & Sugihara, G. (1995). *Int. J. Pept. Protein Res.* **46**, 97–105.

Ando, S., Nishikawa, H., Takiguchi, H., Lee, S. & Sugihara, G. (1993). *Biochim. Biophys. Acta*, **1147**, 42–49.

Bechinger, B. (1999). *Biochim. Biophys. Acta*, **1462**, 157–183.

Burkhart, B. M. & Duax, W. L. (1999). *Nature Struct. Biol.* **6**, 610–611.

Cross, T. A., Arseniev, A., Cornell, B. A., Davis, J. H., Kilian, J. A., Koeppe, R. E. II, Nicholson, R. K., Separovic, F. & Wallace, B. A. (1999). *Nature Struct. Biol.* **6**, 611–612.

DeLano, W. L. (2002). *The PyMOL Molecular Graphics System.* DeLano Scientific, San Carlos, CA, USA. http://www.pymol.org.

Dubos, R. J. (1939*a*). *J. Exp. Med.* **70**, 1–10.

Dubos, R. J. (1939*b*). *J. Exp. Med.* **70**, 11–17.

Dubos, R. J. & Cattaneo, C. (1939). *J. Exp. Med.* **70**, 249–256.

Gause, G. F. & Brazhnikova, M. G. (1944). *Nature (London)*, **154**, 703.

Grotenbreg, G. M., Buizert, A. E. M., Llamas-Saiz, A. L., Spalburg, E., van Hooft, P. A. V., de Neeling, A. J., Noort, D., van Raaij, M. J., van der Marel, G. A., Overkleeft, H. S. & Overhand, M. (2006). *J. Am. Chem. Soc.* **128**, 7559–7565.

Grotenbreg, G. M., Kronemeijer, M., Timmer, M. S., El Oualid, F., van Well, R. M., Verdoes, M., Spalburg, E., van Hooft, P. A., de Neeling, A. J., Noort, D., van Boom, J., van der Marel, G. A., Overkleeft, H. S. & Overhand, M. (2004). *J. Org. Chem.* **69**, 7851–7859.

Grotenbreg, G. M., Spalburg, E., de Neeling, A. J., van der Marel, G. A., Overkleeft, H. S., van Boom, J. H. & Overhand, M. (2003). *Bioorg. Med. Chem.* **11**, 2835–2841.

Grotenbreg, G. M., Timmer, M. S. M., Llamas-Saiz, A. L., Verdoes, M., van der Marel, G. A., van Raaij, M. J., Overkleeft, H. S. & Overhand, M. (2004). *J. Am. Chem. Soc.* **126**, 3444–3446.

Huang, H. W., Chen, F.-Y. & Lee, M.-T. (2004). *Phys. Rev. Lett.* **92**, 198304.

Hull, S. E., Karlsson, R., Main, P., Woolfson, M. M. & Dodson, E. J. (1978). *Nature (London)*, **275**, 206–207.

Jelokhani-Niaraki, M., Kondejewski, L. H., Farmer, S. W., Hancock, R. E. W., Kay, C. M. & Hodges, R. S. (2000). *Biochem. J.* **349**, 747–755.

Kawai, M., Yamamura, H., Tanaka, R., Umemoto, H., Ohmizo, C., Higuchi, S. & Katsu, T. (2005). *J. Pept. Res.* **65**, 98–104.

Kondejewski, L. H., Farmer, S. W., Wishart, D. S., Hancock, R. E. & Hodges, R. S. (1996). *Int. J. Pept. Protein Res.* **47**, 460–466.

Kondejewski, L. H., Farmer, S. W., Wishart, D. S., Kay, C. M., Hancock, R. E. & Hodges, R. S. (1996). *J. Biol. Chem.* **271**, 25261–25268.

Kondejewski, L. H., Lee, D. L., Jelokhani-Niaraki, M., Farmer, S. W., Hancock, R. E. W. & Hodges, R. S. (2002). *J. Biol. Chem.* **277**, 67–74.

Lee, D. L. & Hodges, R. S. (2003). *Biopolymers*, **71**, 28–48.

McInnes, C., Kondejewski, L. H., Hodges, R. S. & Sykes, B. D. (2000). *J. Biol. Chem.* **275**, 14287–14294.

Otwinowski, Z. & Minor, W. (1997). *Methods Enzymol.* **276**, 307–326.

Prenner, E. J., Kiricsi, M., Jelokhani-Niaraki, M., Lewis, R. N. A. H., Hodges, R. S. & McElhaney, R. N. (2005). *J. Biol. Chem.* **280**, 2002–2011.

Prenner, E. J., Lewis, R. N. A. H., Jelokhani-Niaraki, M., Hodges, R. S. & McElhaney, R. N. (2001). *Biochim. Biophys. Acta*, **1510**, 83–92.

Prenner, E. J., Lewis, R. N. A. H. & McElhaney, R. N. (1999). *Biochim. Biophys. Acta*, **1462**, 201–221.

Salgado, J., Grage, S. L., Kondejewski, L. H., Hodges, R., McElhaney, R. N. & Ulrich, A. S. (2000). *Proceedings of the 15th European Experimental NMR Conference, EENC 2000*, 12–17 June 2000, University of Leipzig, Germany, p. 1.

Salgado, J., Grage, S. L., Kondejewski, L. H., Hodges, R. S., McElhaney, R. N. & Ulrich, A. S. (2001). *J. Biomol. NMR*, **21**, 191–208.

Schmidt, G. M. J., Hodgkin, D. C. & Oughton, B. M. (1957). *Biochem. J.* **65**, 744–756.

Sheldrick, G. M. (1998). *SHELX*97. Institüt für Anorganische Chemie der Universität, Göttingen, Germany.

Sheldrick, G. M. (2003). *SADABS* v.2.10. Bruker AXS Inc., Madison, Wisconsin, USA.

Spek, A. L. (2003). *J. Appl. Cryst.* **36**, 7–13.

Tishchenko, G. N., Adrianov, V. I., Vainstein, B. K., Woolfson, M. M. & Dodson, E. (1997). *Acta Cryst.* D**53**, 151–159.

Wallace, B. A. & Janes, R. W. (1991). *J. Mol. Biol.* **217**, 625–627.

Weeks, C. M. & Miller, R. (1999). *J. Appl. Cryst.* **32**, 120–124.

Zhang, L., Rozek, A. & Hancock, R. E. W. (2001). *J. Biol. Chem.* **276**, 35714–35722.